Electrochimica Acta 503 (2024) 144822

Contents lists available at ScienceDirect

Electrochimica Acta

journal homepage: www.journals.elsevier.com/electrochimica-acta

# Dual immunoplatform to assess senescence biomarkers TIMP-1 and GDF-15: Advancing in the understanding of colorectal cancer

Sandra Tejerina-Miranda [a], Maria Gamella [a], María Pedrero [a], Ana Montero-Calle [b], Raquel Rejas [b], José M. Pingarrón [b], Rodrigo Barderas [b,c,*], Susana Campuzano [a,*]

[a] Departamento de Química Analítica, Facultad de CC. Químicas, Universidad Complutense de Madrid, Pza. de las Ciencias 2, Madrid 28040, Spain
[b] Chronic Disease Programme, UFIEC, Institute of Health Carlos III, Majadahonda, Madrid 28220, Spain
[c] CIBER of Frailty and Healthy Aging (CIBERFES), Madrid, Spain

ARTICLE INFO

*Keywords:*
Electrochemical immunoplatforms
Dual determination
Colorectal cancer
Cellular senescence
Plasma
Tissues

ABSTRACT

In this work, we report the development of electrochemical bioplatforms for both the single determination of TIMP-1 and the simultaneous determination of TIMP-1 and GDF-15, two biomarkers of cellular senescence and prognosis in colorectal cancer (CRC). The designed immunoplatforms rely on a sandwich-type configuration labeled with horseradish peroxidase (HRP) built on magnetic microsupports and involve a pair of specific antibodies to capture and detect each target protein. Amperometric readout was performed upon trapping the magnetic bioconjugates on the surface of either single or dual disposable carbon electrodes, using the hydroquinone/hydrogen peroxide ($HQ/H_2O_2$) system. The attractive analytical performance of the TIMP-1 bioplatform, achieving a LOD of 13.0 pg $mL^{-1}$ and a dynamic range between 43.4 and 2500 pg $mL^{-1}$, led us to exploit it for TIMP-1 determination in cell extracts and tissues of CRC samples. The results showed the possibility of discriminating the metastatic capabilities of cells and detecting CRC patients, after just a simple dilution and in only 60 min. The multiplexing feasibility of the developed immunoplatform allowed the implementation of a dual assay for the simultaneous determination of TIMP-1 (LOD 19.2 pg $mL^{-1}$) and GDF-15 (LOD 16.6 pg $mL^{-1}$). The dual platform was used for the analysis of CRC samples (plasma and cell secretomes) in just 75 min and using a very simple protocol. These characteristics make the developed immunoplatform a very attractive tool to face particularly challenging samples, such as secretomes or plasma from CRC patients, due to the required sensitivity, thus providing a better snapshot of CRC.

## 1. Introduction

Advanced age is one prominent risk factor for colon adenoma and colorectal cancer (CRC) through cellular senescence. The aging immune system helps accumulation of senescent cells in tissues which, in turn, may create pro-tumorigenic microenvironments through the senescence-associated secretory phenotype (SASP), characterized by the increased expression of cytokines, chemokines, growth factors, and proteases [1]. Cellular senescence results from endogenous and exogenous dysfunction or damage such as DNA damage, telomere dysfunction, oncogene activation, and organelle stress. It is not only induced by organ aging, but it has also been associated, on the one hand, with tumor suppression, and sometimes with tumor development stimulation and malignant progression. The 2022 edition of cancer hallmarks, a set of functional capabilities crucial for human cells' ability to form malignant tumors, added senescent cells as a new hallmark [2]. Cancer and aging are different manifestations of cellular damage accumulation. Cell damage occasionally confers abnormal benefits to certain cells deriving to cancer, while cellular senescence is caused by a time-dependent accumulation of cellular damage. Both, tumor, and non-tumor cells can undergo senescence [3].

Dong et al. have recently proposed a senescence-related gene prognostic signature to be applied in the classification of CRC patients and guiding of individualized treatment [3]. CRC global incidence and mortality rates ranked third and second, respectively, in the world in 2022, with the number of cases being higher for men compared to women. There were more than 1.1 million (10.7 %) new cases of CRC worldwide and it was responsible for over 500,000 (4.7 %) deaths in 2022. The incidence and mortality cumulative risk was highest in Europe followed by Oceania and Northern America [4]. Regarding

* Corresponding authors.
*E-mail addresses:* r.barderasm@isciii.es (R. Barderas), susanacr@quim.ucm.es (S. Campuzano).

https://doi.org/10.1016/j.electacta.2024.144822
Received 12 June 2024; Received in revised form 22 July 2024; Accepted 1 August 2024
Available online 2 August 2024

patients´ age, CRC is rare before the age of 40, yet its incidence increases significantly between the ages of 40 and 50 and is enhanced in each subsequent decade [5]. Local treatments, more useful for earlier cancer stages, such as surgery, ablation, and embolization or radiation therapy, can be combined at the same time or used after systemic treatments such as chemotherapy, targeted therapy drugs, and immunotherapy, depending on the stage of cancer [6]. A large majority of patients with advanced CRC suffer from a poor therapeutic outcome with higher rates of malignant recurrence and distant metastases, resulting in a 5-year survival rate of less than 10 % [7]. Hence, it is particularly important to find a prognostic model that can accurately classify CRC patients, so that appropriate treatment can be selected as a function of CRC stage. Moreover, cost-effectiveness would be enhanced by early CRC diagnosis and prognosis methods as they would avoid long and expensive cancer treatments. Actual screening methods for CRC include [6]: stool-based tests such as Fecal Immunochemical Test (FIT) that although less invasive and easier to be done more often possesses a low sensitivity; visual (structural) exams such as colonoscopy, which look at the structure of the colon and rectum for any abnormal areas, either with a scope put into the rectum, or with special imaging (X-ray) tests; these tests can be done less often than stool-based tests, but they require more preparation ahead of time, and can have some risks not seen with stool-based tests. A screening algorithm combining FIT, blood-based biomarkers, and demographics has been recently proposed as a less invasive way to screen CRC without reducing the high sensitivity of colonoscopy [8].

Plasmatic levels of growth differentiation factor 15 (GDF-15), an inflammation-related biomarker, and tissue inhibitor of metalloproteinase 1 (TIMP-1), an extracellular matrix turnover biomarker, have been shown to be influenced by dynamic contribution of non-cardiac tissues reflecting stress in other organs than heart, either as a consequence of the failing heart and/or of other distinct pathophysiological pathways and underlying morbidities, like metabolic syndromes, metastatic melanoma, gait speed decline in adults from middle to older age, etc. [9–13]. GDF-15, inducing proliferation, stemness, invasion, and metastasis in tumor cells and regarded as probable stimulator of angiogenesis in malignant neoplasms, is considered a promising diagnostic and prognostic biomarker in CRC [14,15]. In fact, increased levels of this biomarker have been found in serum and plasma of CRC patients compared to healthy individuals [16–18] and in tumor tissues compared to margin tissues of CRC patients [14,15]. Also, as reported by Guo et al. [1] senescent fibroblasts and GDF-15 induce physiological and molecular changes that promote adenoma-adenocarcinoma initiation and progression in the colon. On the other hand, TIMP-1 levels in serum can differentiate between CRC and colorectal adenomas (CA) and have been shown as correlated with cancer progression, while an increased plasma level of this biomarker constitutes a significant prognostic factor for the survival of patients with CRC [19–21]. A decrease in TIMP-1 levels activates matrix metalloproteinases (MMPs) when the SASP of senescent tumor cells is reprogrammed, thus promoting metastasis [22]. Also, treatment with 4′-demethyldeoxypodophyllotoxin glucoside (4-DPG), a natural podophyllotoxin analogue, attenuates epithelial–mesenchymal transition (EMT), which is critical for the metastatic dissemination of cancer cells together with deriving in an increase in epithelial markers such as TIMP-1 [23].

Considering all this background, the availability of technologies that allow the determination of these two biomarkers both individually and simultaneously in the tumor microenvironment, is considered of great interest to delve deeper into the role they play in cellular senescence and CRC progression as well as in the relationship between these processes, key aspects to continue advancing in its understanding and treatment. Both biomarkers are generally determined using enzyme-linked immunoassays (ELISAs) [24–32], Western Blot [30,33], or quantitative reverse transcriptase–polymerase chain reaction (RT-PCR) [30,34]. Other methods such as surface plasmon resonance (SPR) have also been used for their determination [35–37]. However, none of them fully meet the demands of today's clinic in terms of simplicity, affordable cost, multiplexing compatibility, and point-of-care applicability. These limitations are what increasingly highlight the potential of technologies based on electrochemical biosensing, which in recent years have demonstrated their competitiveness for multiple determination, even at different molecular levels, and to face particularly challenging samples to learn more about the tumor microenvironment such as the cell secretome [38–40]. According to the state of the art, few electrochemical immunoplatforms have been reported for the determination of GDF-15. Some of them involve the use of elaborated nanocomposites as the secondary antibody labels which needs long-lasting preparation procedures [41–43], and/or as working electrode surface modifiers [41–44]. Very recently, we have reported an immunoplatform that combines the advantages of using magnetic beads (MBs) [45] and amperometric transduction at screen-printed electrodes (SPCEs) to stand out in terms of simplicity and reduced testing time, which are key aspects for routine and *in situ* applications [18]. Regarding TIMP-1, to our knowledge, no electrochemical systems have been reported till now for its determination. Considering this background, in this paper we report the development and implementation of a simple and reliable electrochemical immunoplatform for the determination of TIMP-1 in clinical samples. Moreover, the possibility of carrying out dual simultaneous analysis of GDF-15 and TIMP-1 by immune-attaching both targets to modified MBs which are then captured on dual SPCEs to undergo amperometric transduction using the $H_2O_2$/peroxidase (HRP)/hydroquinone (HQ) electrochemical system, is evaluated.

## 2. Experimental part

"Apparatus and electrodes" and "Reagents and solutions" are available in the Supplementary Material.

### 2.1. Sandwich immunoassay implementation on MBs

The HOOC-MBs modification consisted of several incubation and washing steps carried out in 1.5 mL microcentrifuge tubes. The incubation steps were performed in a Thermoshaker at 25 °C under constant stirring (950 rpm) using 25 μL of the corresponding solution, whereas the washing steps, made at the end of each incubation step, were accomplished with 50 μL of the appropriate solution keeping the microcentrifuge tubes in a magnetic concentrator for 2 min to carefully remove the supernatant.

The implementation of the TIMP-1 sandwich immunoassay consisted of, first, placing 3 μL-aliquots of the HOOC-MBs suspension in the microcentrifuge tubes and washing twice with MES buffer for 10 min. Then, the activation of the MBs-carboxyl groups was carried out by incubating the microparticles with a freshly prepared EDC/Sulfo-NHS solution for 35 min, followed by two washing steps with MES buffer. The activated HOOC-MBs were incubated with a 25 μg $mL^{-1}$ $CAb_{TIMP\text{-}1}$ solution prepared in MES buffer for 2.5 min. Thereafter, the $CAb_{TIMP\text{-}1}$−MBs were washed twice with MES buffer and incubated in 1.0 M ETA solution for 60 min to block the remaining activated carboxylic groups. Subsequently, the modified MBs were washed once with 0.1 M Tris–HCl buffer (pH 7.2) and twice with BB solution. At this point, the $CAb_{TIMP\text{-}1}$−MBs can be used to perform the assay or stored in filtered PBS at 4 °C for further use.

The formation of the HRP-labelled sandwich immunocomplexes required only a single 1-h incubation step in a mixture solution composed of TIMP-1 standard (or the sample to be analyzed), 1.0 μg $mL^{-1}$ b-$DAb_{TIMP\text{-}1,}$ and 1/1000 diluted Strep-HRP, prepared in BB. Finally, the magnetic bioconjugates were washed twice with BB and resuspended in 50 μL of PB pH 6.0 for single determination.

The developed TIMP-1 immunoassay was also implemented in a dual platform for the simultaneous determination of TIMP-1 and GDF-15. The preparation of the immunoconjugates for the determination of GDF-15 was performed according to that previously reported [18]. No changes with respect to the single determination were made to carry out the dual

determination in terms of concentration, immunoreagent, or incubation times but, once prepared, both magnetic immunoconjugates were resuspended in 5 μL of PB pH 6.0 to perform the amperometric transduction.

### 2.2. Amperometric measurements

A SPCE or a SPdCE was placed in the appropriate homemade PMMA casing containing either one (for the single determination) or two (for the simultaneous determination) embedded neodymium magnet/s. The modified MBs (resuspended in 50 or 5 μL depending on whether the measurement was single or dual, respectively) were dropped and trapped on the surface of the working electrode/s.

Once the SPCE (or SPdCE)/PMMA casing set was connected to the potentiostat, using the appropriated cable, it was immersed in an electrochemical cell containing 10 mL of 1.0 mmol $l^{-1}$ HQ solution prepared in PB buffer pH 6.0. Amperometric detection was carried out by applying a constant potential of – 0.20 V (*vs.* the Ag *pseudo*-reference electrode) under continuous stirring. After the stabilization of the background current, 50 μL of a freshly prepared 0.1 mol $l^{-1}$ $H_2O_2$ solution were added to the cell producing a cathodic current variation due to the HQ-mediated enzymatic reduction of $H_2O_2$ which was proportional to the analyte concentration. The signals reported in this work were obtained by calculating the difference between the steady-state current (once the $H_2O_2$ was added), and the background current (in the absence of $H_2O_2$), and they are the mean values of three replicates. The error bars displayed in the figures were estimated as the standard deviation of the replicates.

### 2.3. Analysis of CRC samples

Cell extracts, secretomes, and plasma from healthy individuals and CRC patients as well as paired CRC tumoral and non-tumoral tissue samples were analyzed. Extracts and secretomes of 5 different CRC cells, plasma samples from 2 healthy subjects and 4 patients with advanced CRC (2 in stage III and 2 in stage IV), and paired tissue samples from 8 patients with advanced CRC (4 in stage III and 4 in stage IV) were analyzed.

Two isogenic CRC cell models with different metastatic abilities were used: the KM12 cell system, obtained from the I. Fidler's laboratory (MD Anderson Cancer Center), composed by the poorly metastatic KM12C cells and the highly metastatic to liver KM12SM and to liver and lung KM12L4a cells; the SW cell system, obtained from the American Type Culture Collection (ATCC) repository, composed by the low metastatic SW480 cells and the highly metastatic to lymphatic nodes SW620 cells. The cells were grown at confluency and the protein extracts obtained as previously reported [39,46] and stored at − 80 °C until use. The concentration (in μg $\mu L^{-1}$) of the extracts was determined using the tryptophan method [47] and the desired protein amount was analyzed by diluting the appropriate volume in the corresponding buffer. Additionally, secretome samples were centrifuged 5 min at 1200 rpm and 4 °C. Then, supernatants were transferred to a new tube and pellets were discarded.

Patients gave written informed consent to participate in the research. Samples were provided by the biobank of the San Carlos Clinical Hospital after approval by the Ethical Review Committee (CEI PI 13_2020-v2). All samples were stored at – 80 °C and used in accordance with all ethical aspects, relevant guidelines, and regulations for both sample handling and experiments conducting.

After a careful statistical analysis for all the analyzed samples no matrix effect was observed. Therefore, the concentrations of both proteins were calculated by interpolating the current values measured for the samples into the calibration plots constructed with standard solutions. The single quantification of TIMP-1 in tissue samples and cell extracts was accomplished through a calibration for TIMP-1 over the 0 to 2000 pg $mL^{-1}$ concentration range and using 0.10 and 0.25 μg of tissue samples and cell extracts, respectively.

Plasma and cell secretome samples were analyzed with the dual platform for the simultaneous determination of GDF-15 and TIMP-1. The analysis required either 1/25 or 1/250 sample dilution for GDF-15 and TIMP-1, respectively. The sample signals were interpolated into calibration plots over the 0 to 1000 pg $mL^{-1}$ concentration range of standard proteins.

### 2.4. Immunoblotting analysis of cellular samples

CRC cell protein extracts and secretomes were also analyzed by Western Blot to determine TIMP-1. For Western Blotting, 10 μg of each cell extract were separated by 10 % PAGE-SDS and transferred to a nitrocellulose membrane (100 V, 90 min). Subsequently, membranes were incubated with a mouse anti-TIMP-1 (DY970, R&D system) or a mouse anti-GAPDH (sc-47724, Santa Cruz Biotechnology, Texas, USA) antibody 1/1000 diluted in 3 % BSA or in 3 % skimmed milk in 0.1 % PBS-Tween-20, respectively, followed by incubation with a HRP-labelled goat anti-mouse IgG secondary antibody (A9044, Merck, Frankfurt, Germany). Chemiluminescence signals were developed using the enhanced chemiluminescence (ECL) Western Blotting substrate (Thermo Fisher Scientific, Waltham, MA, USA), and signals were recorded on an Amersham Image Quant 800 (GE Healthcare, Chicago, IL, USA). Protein band intensities were quantified using ImageJ Software and normalized using GAPDH as loading control.

For the analysis of secretome samples, 50 μL of each sample were transferred to a nitrocellulose membrane using a Bio-Dot Microfiltration System (Bio-Rad, California, USA) and incubated with the anti-TIMP-1 antibody as previously described.

### 2.5. Statistical analysis

All experiments were performed by triplicate. ROC curves were obtained to determine the diagnostic capacity of TIMP-1 and GDF-15 using the pROC package in RStudio. T-tests were obtained with RStudio. A p-value $< 0.05$ was considered statistically significant.

## 3. Results and discussion

Before developing a dual electrochemical immunoplatform for the simultaneous determination of TIMP-1 and GDF-15 and given that to date no bioplatforms have been reported for the determination of TIMP-1, we first proceeded to develop an amperometric immunoplatform for the single determination of this biomarker.

Scheme 1 illustrates the steps and fundamentals involved for the construction of the single and dual immunoplatforms through the implementation of sandwich immunocomplexes using capture and biotinylated antibodies, specific to each target analyte, and a Strep-HRP conjugate as label. Thereafter, the bioconjugates were captured either on the working electrode (WE) surface of the single SPCEs for the individual determination of TIMP-1, or on SPdCE WEs, to perform the simultaneous determination of GDF-15 and TIMP-1. Amperometric readings at – 0.20 V (*vs* Ag *pseudo*-reference electrode) after the addition of $H_2O_2$ in the presence of HQ were used to quantify both proteins.

### 3.1. Optimization of experimental variables for TIMP-1 analysis

The experimental variables involved in the preparation of TIMP-1 sandwich immunocomplexes on HOOC-MBs were optimized using single SPCEs. The selection criterion was larger target-to-blank ratios (T/B) achieved when measuring amperometric responses either in the presence of a fixed TIMP-1 concentration (1000 pg $mL^{-1}$, T) or in its absence (B). The results achieved for the optimization of the different parameters that encompass the preparation of the TIMP-1 immunoconjugates are shown in Fig. 1 and summarized in Table 1.

It is important to emphasize that, according to the rationale of the

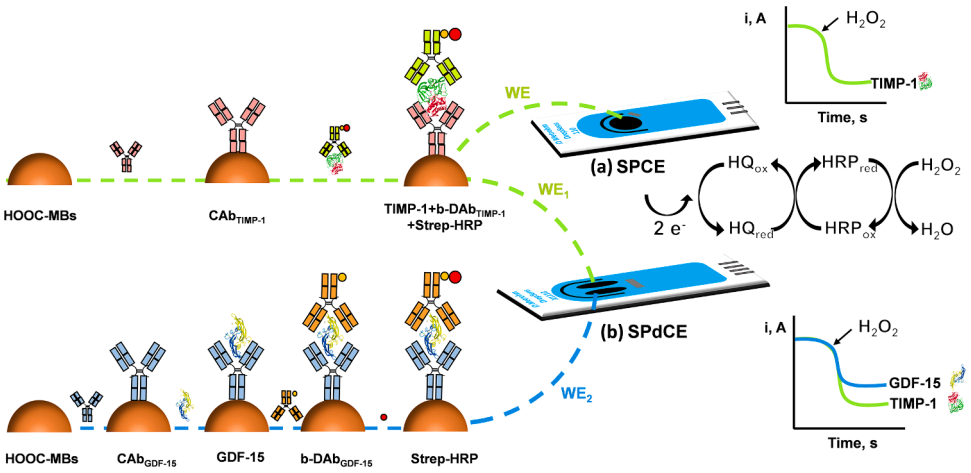


**Scheme 1.** Schematic diagram showing the steps required for preparing the HRP-labelled sandwich bioconjugates for the single determination of TIMP-1 at SPCEs (a), and the simultaneous determination of GDF-15 and TIMP-1 at SPdCEs (b), by means of amperometric transduction in the presence of $H_2O_2$ and HQ.

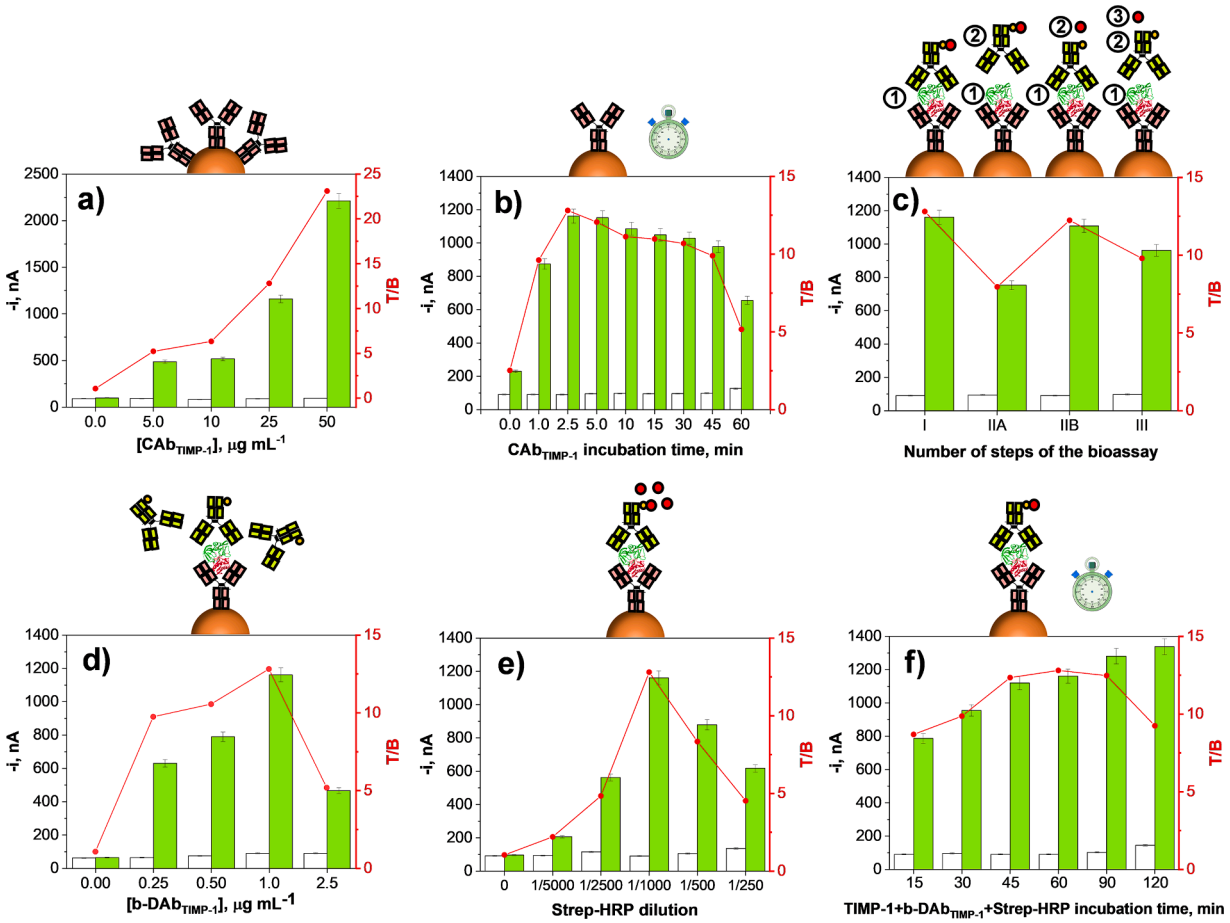


**Fig. 1.** Dependence of the amperometric responses provided by the developed bioplatform for the single determination of TIMP-1 in the absence (white bars, B) and in the presence of 1000 pg mL$^{-1}$ TIMP-1 (green bars, T), and the resulting T/B ratio values (red dots and line) with the concentration (a) and incubation time (b) of the $CAb_{TIMP-1}$ solution, number of steps involved to form the sandwich immunocomplexes (c), concentration of the b-$DAb_{TIMP-1}$ solution (d), dilution of the Strep-HRP solution (e), and incubation time of the TIMP-1/b-$DAb_{TIMP-1}$/Strep-HRP mixture solution (f).

immunoassay, it was not possible to detect the analyte in the absence of $CAb_{TIMP-1}$ (Fig. 1**a,** bars 0). As it can be seen in Fig. 1**a**, a concentration of $CAb_{TIMP-1}$ of 50 μg mL$^{-1}$ provided a larger T/B ratio. However, a 25 μg mL$^{-1}$ $CAb_{TIMP-1}$ concentration was selected for further work because the achieved T/B ratio was sufficient for the determination of TIMP-1 and the cost of the assay is largely reduced. Importantly, a better T/B ratio was found for an incubation time to immobilize the $CAb_{TIMP-1}$ as short as 2.5 min. The T/B ratio decreased for longer incubation times (Fig. 1**b**), due to a lower efficiency in the target antigen recognition because of sterically hindrance effects [48].

Next, the number of steps involved in the construction of the immunoplatform were evaluated by testing different protocols involving

**Table 1**
Optimizations of the key experimental variables involved in the development of the immunoplatform for the single determination of TIMP-1.

| Variable* | Tested Range | Selected value |
|---|---|---|
| [$CAb_{TIMP-1}$], μg $mL^{-1}$ | 0.0–50.0 | 25.0 |
| $CAb_{TIMP-1}$ incubation time, min | 0–60 | 2.5 |
| Number of assay steps | 1–3 | 1 |
| [b-$DAb_{TIMP-1}$], μg $mL^{-1}$ | 0–2.5 | 1.0 |
| Strep-HRP dilution | 0–1/250 | 1/1000 |
| TIMP-1 + *b*-DAb+Strep-HRP Incubation time, min | 15–120 | 60 |

* Experimental variables involved in the detection step, such as the applied potential, $H_2O_2$ and HQ concentrations, as well as the pH and composition of the supporting electrolyte were optimized previously [49].

different 30 min incubation steps starting from the $CAb_{TIMP-1}$−MBs preparation (Fig. 1**c**). The assayed protocols were: protocol I, the bioconjugates were built in a single incubation step with a mixture solution containing TIMP-1, b-$DAb_{TIMP-1}$ and Strep-HRP (Fig. 1**c, bars I**); protocols IIA and IIB consisting of two successive steps; whereas in protocol IIA a first incubation step was made in the protein standard solution and a second one in a solution containing b-$DAb_{TIMP-1}$ and Strep-HRP (Fig. 1**c, bars IIA)**, protocol IIB involved a first incubation with a mixture solution of TIMP-1 and b-$DAb_{TIMP-1}$ followed by a second incubation in the Strep-HRP solution (Fig. 1**c, bars IIB**); in protocol III, three sequential incubation steps with TIMP-1, b-$DAb_{TIMP-1}$ and the Strep-HRP conjugate solution were carried out (Fig. 1**c, bars III**). As it can be seen, a larger T/B ratio was obtained for protocol I, which also implied a shorter assay time: Therefore, protocol I was selected for the development of the immunoplatform.

With respect to the optimization of the b-$DAb_{TIMP-1}$ concentration (Fig. 1**d**) and the Strep-HRP conjugate dilution (Fig. 1**e**), the T/B ratios peaked for values of 1 μg $mL^{-1}$ and 1/1000, respectively. A decrease in both T/B ratios was apparent for higher concentrations, mainly due to a decrease in the specific signal probably as a result of agglutination phenomena in the immunoreagents mixture solution. The incubation time of the $CAb_{TIMP-1}$−MBs with the TIMP-1, b-$DAb_{TIMP-1}$ and Strep-HRP mixture also tested. Although the signal in the presence of TIMP-1 increased with the incubation time up to 120 min, the increase in the non-specific adsorptions shown in Fig. 1**f** gave rise to a better T/B for an incubation time of 1 h.

### *3.2. Analytical performance of the immunoplatform for the determination of TIMP-1*

The calibration plot for TIMP-1 displayed in Fig. 2 showed a linear dependence between the amperometric signals and the target biomarker concentration from 43 to 2500 pg $mL^{-1}$ ($R^2$= 0.996, and fitted to the equation − i, nA= (1.16 ± 0.03) nA mL $pg^{-1}$ [TIMP-1] + (70 ± 36) nA. A limit of detection (LOD) of 13.01 pg $mL^{-1}$ was calculated according to the 3 × $s_b$/m criteria (where $s_b$ is the standard deviation of 10 measurements for the blank solution and m is the slope of the calibration curve), which is far below the clinical threshold stablished in serum for CRC diagnosis (200–600 ng $mL^{-1}$ [25,31,50]). A relative standard deviation (RSD) of 3.6 % was obtained from the amperometric measurements provided by 10 different bioconjugates prepared the same day, thus confirming the good reproducibility of the assay.

Although the determination of TIMP-1 can be performed by immunohistochemistry [51], or ELISA [27-29], biosensors provide an alternative to these hardly portable methods, which imply mostly high-cost and time-consuming procedures [52]. Regarding the determination of TIMP-1, O'Connor et al. developed an ECL sandwich immunoassay using CdSeS QDs as ECL emitters, reaching a LOD of 1.54 ng $mL^{-1}$ [53], which is significantly higher than that the achieved in this work (13.01 pg $mL^{-1}$). In addition, the method was not applied to the analysis of real samples. The detection of TIMP-1 was also reported exploiting the use of ECL

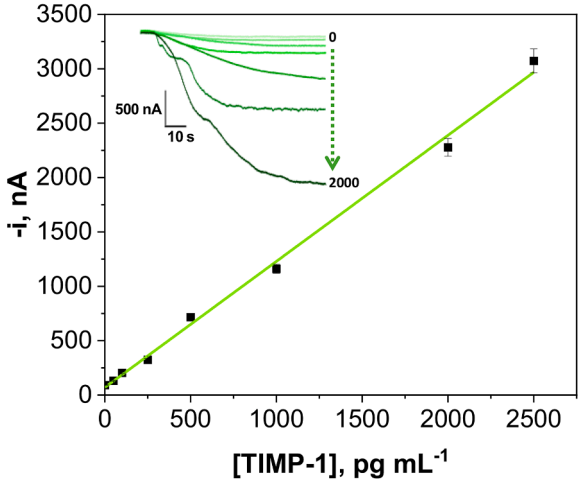


**Fig. 2.** Calibration graph constructed using the immunoplatform developed for the single determination of TIMP-1. Inset: amperometric traces recorded for 0, 50, 100, 250, 500, 1000 and 2000 pg $mL^{-1}$.

imaging, but it was performed at a single concentration of 100 ng $mL^{-1}$ [54]. A biosensing system involving surface plasmon resonance imaging (SPRI) was reported by Gorodkiewicz's group for the determination of TIMP-1 in plasma samples of bladder cancer patients, claiming a LOD of 9 pg $mL^{-1}$ [35]. This value is similar to that achieved with the developed immunoplatform, but the method required more complex and non-portable equipment thus limiting its applicability for onsite detection. Moreover, a label surface acoustic wave immunosensor for the determination of TIMP-1 was reported [55], reaching a LOD value of 2 ng $mL^{-1}$ below the clinical cut-off value established for breast cancer. However, the immunosensor was not applied to real samples. In this context, the immunoplatform developed in this work stands up as an interesting candidate to perform the proposed determination due to its great sensitivity, ease of operation, low manufacturing cost and possibility of in field operation.

To shorten the assay, the storage stability of the $CAb_{TIMP-1}$−MBs immunoconjugates once blocked with ethanolamine was tested by resuspending and keeping them in filtered PBS at 4 °C until used. The amperometric responses obtained in the absence and in the presence of 1000 pg $mL^{-1}$ TIMP-1 showed T/B ratios within the set control values for at least 28 days (**Fig. S1** in the Supplementary Material).

The selectivity of the developed bioplatform was tested by comparing the amperometric response measured for 0 (white bars, B) and 1000 pg $mL^{-1}$ TIMP-1 (color striped bars, T) in the presence of some potential interfering proteins which can be found in human serum or plasma, such as hIgG (yellow striped bars), Hb (red striped bars), HSA (purple striped bars) and TNFα (blue striped bars) at concentrations of 1 mg $mL^{-1}$, 5 mg $mL^{-1}$, 50 mg $mL^{-1}$ and 10 ng $mL^{-1}$, respectively, or 1/10, 1/100 or 1/1000 diluted, if necessary (Fig. 3). In addition, the supplier company of the DY970 DuoSet ELISA Human TIMP-1 certified no cross-reactivity for recombinant human MMP-1, MMP-2, MMP-3, and TIMP-2 and for recombinant mouse TIMP-1 at tested concentrations of 50 ng $mL^{-1}$.

As shown in Fig. 3, among all the tested potential interferences, Hb and HSA showed an interference at the largest concentrations tested (5 mg $mL^{-1}$ and 50 mg $mL^{-1}$, respectively). Hb interference is attributed to its positive association with TIMP-1, as well as to its peroxidase activity [56,57]. The HSA interference was observed in other sandwich immunoassays, especially for concentrations larger than 5 mg $mL^{-1}$ and was attributed to the fact that it can contain IgG of a wide range of specificities that can alter the assay when it is not highly purified [38]. Nevertheless, these interferences were minimized by 100-fold and 1000-fold dilution of Hb and HSA, respectively. It should be noted that

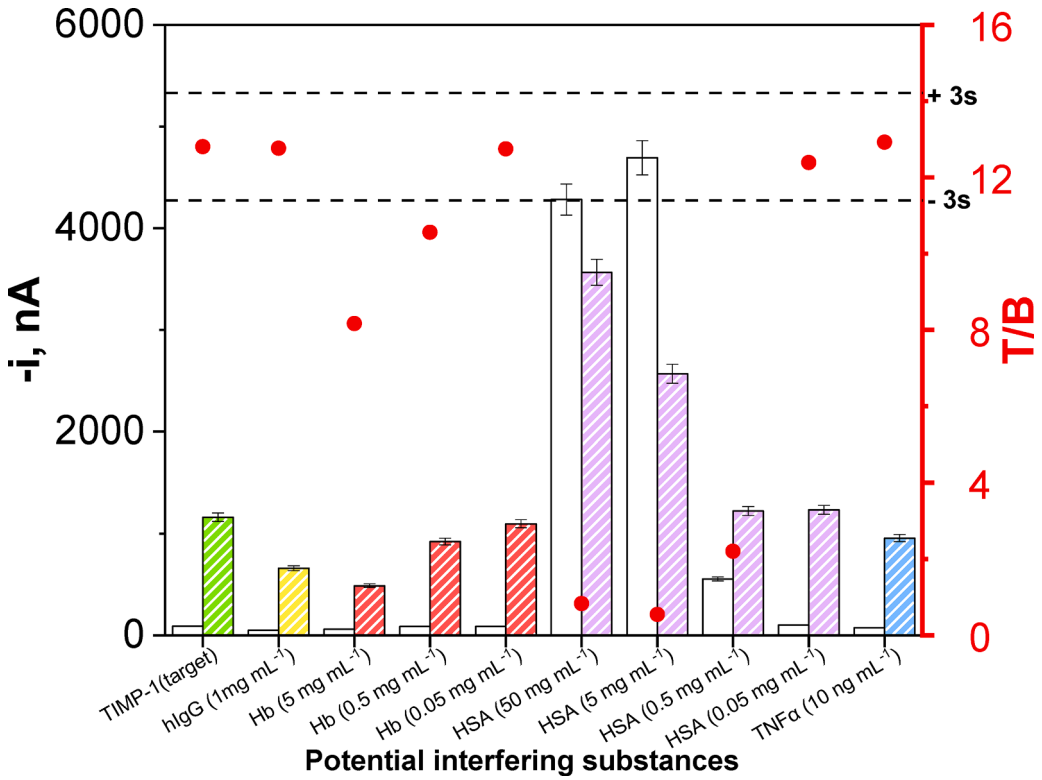


**Fig. 3.** Amperometric responses provided by the developed bioplatform for the determination of TIMP-1 for 0 (white bars) and 1000 pg $mL^{-1}$ TIMP-1 (colored bars) standards prepared in the absence and in the presence of hIgG (1 mg $mL^{-1}$, yellow striped bars), Hb (5, 0.5 and 0.05 mg $mL^{-1}$, red striped bars), HSA (50, 5, 0.5 and 0.05 mg $mL^{-1}$, purple striped bars) and TNFα (10 ng $mL^{-1}$, blue striped bars). T/B ratio values are displayed in red dots and control limits (dashed black lines) were set as ± 3 s of the mean value obtained employing three different immunoplatforms.

the presence and concentration of these potential interferents will depend on the nature of the analyzed samples.

### *3.3. Implementation and assessment of a dual immunoplatform for the simultaneous determination of TIMP-1 and GDF-15*

As it is well-accepted that the use of a single biomarker is unlikely to provide a comprehensive diagnosis, and considering the achieved results obtained with the previously developed immunoplatform for the determination of GDF-15 [18], the simultaneous determination of these biomarkers, both related to cellular senescence and CRC prognosis, was accomplished. This was made through the preparation of independent immunocomplexes batches for each target protein and their capture on the corresponding working electrode of SPdCEs. It is important to remark that no modifications in terms of immunoreagents concentration and incubation times were needed to implement the dual immunoplatform for the determination of TIMP-1 or for GDF-15 [18].

The possible crosstalk between the SPdCE adjacent working

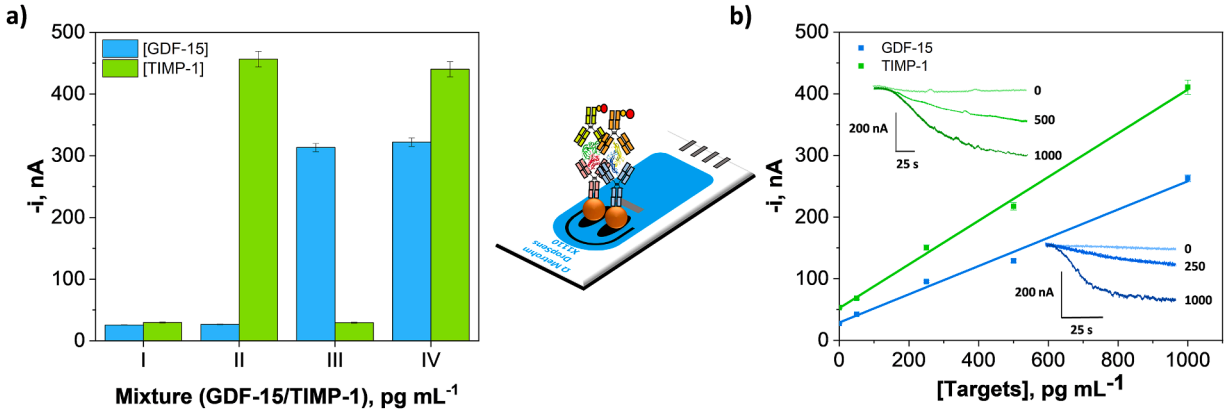


**Fig. 4.** Amperometric responses obtained with the MBs-based dual immunoplatform for the simultaneous determination of GDF-15 and TIMP-1 for mixture solutions containing: 0 pg $mL^{-1}$ of both biomarkers (I); 0 pg $mL^{-1}$ GDF-15 and 1000 pg $mL^{-1}$ TIMP-1 (II); 2500 pg $mL^{-1}$ GDF-15 and 0 pg $mL^{-1}$ TIMP-1 (III), and 2500 pg $mL^{-1}$ GDF-15 and 1000 in pg $mL^{-1}$ TIMP-1 (a); calibration graphs (and real amperometric traces) obtained with the dual immunoplatform for the simultaneous amperometric determination of GDF-15 and TIMP-1 standards (b).

electrodes was evaluated by comparing the amperometric responses for both targets using independent sets of immunoconjugates prepared at different concentrations of TIMP-1 and GDF-15. The results shown in Fig. 4**a** confirmed the absence of cross-reactivity between adjacent electrodes as green bars in experiments II and IV and blue bars in experiments III and IV were not significantly different. Therefore, the dual immunoplatform resulted appropriate for the simultaneous determination of both biomarkers showing also an excellent selectivity of the antibodies towards the tested analytes.

The analytical and operational characteristics of the developed dual immunoplatform are summarized in Table 2. The respective calibration plots were constructed using the experimental parameters given in Table 1 for TIMP-1, and those previously reported by Tejerina-Miranda et al. [18] for GDF-15 (Fig. 4**b**).

As expected, the calculated LODs values were slightly higher than those obtained with the single immunoplatforms, which is attributable both to the smaller surface area of the SPdCEs compared to the SPCEs working electrodes and to the larger diffusion barrier on the working electrode surface by capturing the same amount of MBs on a smaller surface [58]. Nevertheless, the LODs were still far below the clinical serum cut-off values found in the literature for GDF-15 and TIMP-1 (around 1000 pg $mL^{-1}$ [59,60] and 200–600 ng $mL^{-1}$ [23,31,50], respectively) to diagnose CRC. Due to the great importance of these biomarkers for the prognosis of numerous diseases, mainly cardiovascular and oncological, some electrochemical immunosensors and immunoassays were reported for their single determination. So, the reported electrochemical immunosensors to determine GDF-15 claimed similar or even better sensitivities than that achieved in this work [41–44]. However, such methods involved time-consuming processes for the preparation of nanomaterials. In addition, the sensitivity obtained for TIMP-1 with the dual platform is still better than that of the ECL platform reported by O'Coonor et al. [53]. Finally, it is worth highlighting that, to date, this is the first developed bioplatform able to determine both biomarkers simultaneously, which implies a shorter and simpler assay, compatible with clinical applications.

The reproducibility of the measurements made with the dual platform was checked by comparing the amperometric responses obtained by ten different immunoconjugates constructed on the same day for 500 pg $mL^{-1}$ of both biomarkers. RSD values of 2.1 and 2.8 % were obtained for GDF-15 and TIMP-1, respectively, thus verifying the high reproducibility of the employed methodologies both to prepare the immunocomplexes, their capture on the WEs of SPdCEs, and the dual amperometric transduction.

### 3.4. Application of the developed immunoplatforms to the analysis of clinical samples

#### 3.4.1. Individual analysis of TIMP-1

The applicability of the immunoplatform developed for the single determination of TIMP-1 was tested through the analysis of two different types of clinical samples: extracts from metastatic (M: SW620, KM12L4a, and KM12SM) and non-metastatic (NM: SW480 and KM12C) CRC cells and paired tissue extracts (tumoral (T) and margin non-tumoral (NT)) of 8 patients with advanced CRC (4 in stage III and 4 in stage IV).

**Table 2**
Analytical characteristics provided by the developed dual immunoplatform for the simultaneous amperometric determination of GDF-15 and TIMP-1.

| Parameter | GDF-15 | TIMP-1 |
|---|---|---|
| Linear range, pg $mL^{-1}$ | 55–1000 | 64–1000 |
| Slope, nA mL $pg^{-1}$ | 0.23 ± 0.01 | 0.35 ± 0.01 |
| Intercept, nA | 29 ± 7 | 52 ± 6 |
| LOD*, pg $mL^{-1}$ | 16.6 | 19.2 |

* Values estimated according to the 3 × $s_b$/m criterion.

First, the evaluation of the possible matrix effect in the assayed clinical samples was checked. A statistical comparison of the slope values corresponding to the calibration plots prepared with TIMP-1 standard solutions and by spiking representative samples with the protein standard was carried out. The results shown in Table S1 (in the Supplementary Material) indicated that no apparent matrix effect was produced ($t_{exp} < t_{tab}$) in any of the assayed samples when 0.25 μg of protein cell extracts, and 0.10 μg of tissue extracts were analyzed. Therefore, the determination of TIMP-1 in the samples was carried out by interpolation of the amperometric responses for the diluted sample into the external calibration plot constructed with different concentrations of the standard (Fig. 3).

The results for the analysis of extracts from CRC cells with different metastatic potential using the developed TIMP-1 immunoplatform are displayed in Fig. 5a and summarized in Table S2 (in the Supplementary Material). As it can be seen, TIMP-1 was overexpressed in metastatic CRC cells (SW620 and KM12L4a/KM12SM) compared to the respective isogenic non-metastatic counterparts (SW480 and KM12C), in agreement with the results obtained by Western Blot for the same samples (Fig. 6a) and with previously reported data [61] according to which the marked difference in TIMP-1 protein expression between SW480 and SW620 cell lines seems likely to be one factor responsible for phenotypic differences in this model of tumor progression.

Regarding paired CRC tissue samples (T and NT from stages III and IV of the disease), the levels of TIMP-1 (Fig. 5**b** and **Table S3** in the Supplementary Material) were higher in T than in NT tissue samples in agreement with that reported for T tissues of breast [62–64], lung [65], gastric [66,67], and colorectal [33,68,69] cancer patients, which has been associated with poor prognosis of the disease [61,70]. In addition, the concentration of TIMP-1 found in T (median 35.0, range 27 to 320 pg $\mu g^{-1}$) and NT (median 10.8, range 5 to 20 pg $\mu g^{-1}$) tissues agrees with that reported in the literature for gastric cancer [67]. Moreover, the TIMP-1 concentrations found in T tissue for patients in stage III and stage IV of the disease were not significantly different, as reported by Yoshikawa et al. for gastric cancer [66].

Moreover, recovery studies were performed to check the accuracy of the results obtained with the developed bioplatform. These studies were made by spiking representatives from each group of samples with 250 pg $mL^{-1}$ of TIMP-1 standard and following the same protocol as for the non-supplemented samples. The obtained recovery values, upon the subtraction of the endogenous content found in each sample from the overall concentration determined after sample spiking, between 99 and 103 % (Table S4 in the Supplementary Material), proved the reliability of the results provided by the developed immunoplatform for the determination of TIMP-1 in the analyzed samples. The obtained results highlight the potential of the developed immunoplatform, which allows the determination of TIMP-1 in the analyzed samples in only 1 h starting from the prepared $CAb_{TIMP-1}$-MBs, and, therefore, making the immunoplatform very competitive *versus* other available techniques such as ELISA and Western Blot.

#### 3.4.2. Simultaneous analysis of TIMP-1 and GDF-15

Once the viability of the new immunoplatform for the single determination of TIMP-1 in different biological samples was proven, the feasibility of simultaneously determining GDF-15 and TIMP-1 in biological samples in a single run was tested by analyzing 5 secretomes of CRC cells and 6 plasma samples from different individuals (2 healthy, 2 CRC (III), and 2 CRC (IV)). Considering that the GDF-15 analysis in secretome samples had not been previously performed, the possible existence of matrix effect was evaluated. As it is summarized in **Table S5** (in the Supplementary Material), no matrix effect was apparent ($t_{exp} < t_{tab}$) upon a 25-fold dilution. Thus, the simultaneous determination of TIMP-1 and GDF-15 in cell secretome samples was also made by simple interpolation of the current signals measured for the diluted samples into the calibration plots constructed with buffered standards. As it can be seen in Fig. 7, increased GDF-15 levels were observed for metastatic

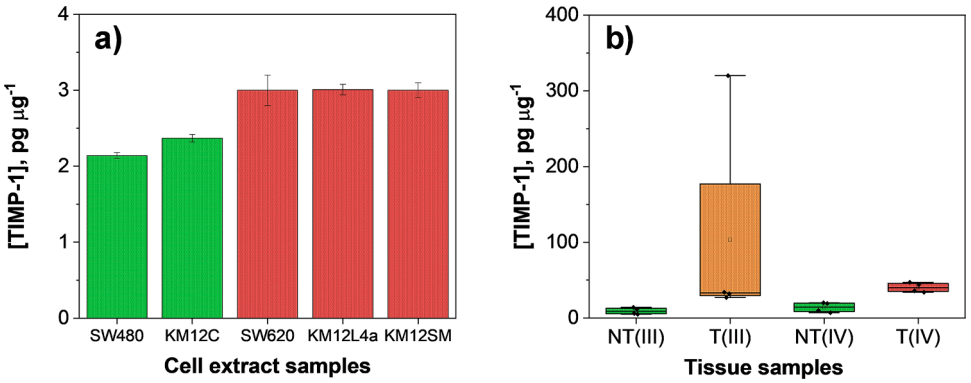


**Fig. 5.** TIMP-1 concentrations determined by using the developed immunoplatform in 0.25 µg of extracts from NM (green) and M (red) CRC cells (a) and 0.10 µg of extracts from T (stage III in orange and stage IV in red) and NT (in green) margin tissues (b).

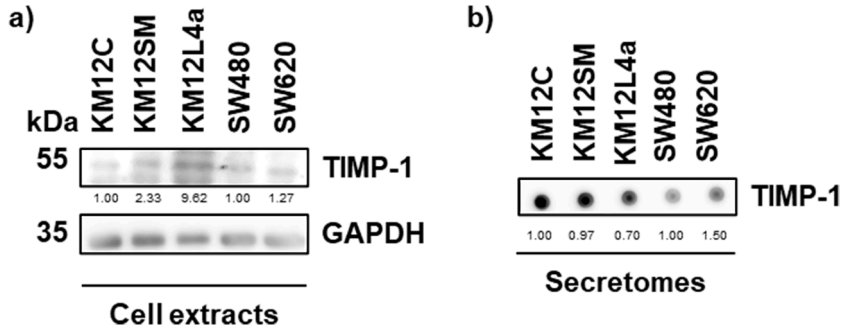


**Fig. 6.** Immunoblotting analysis of TIMP-1 expression in CRC cell protein extracts (a) and secretomes (b). TIMP-1 protein bands of cell extracts were normalized according to GAPDH expression with the ImageJ software.

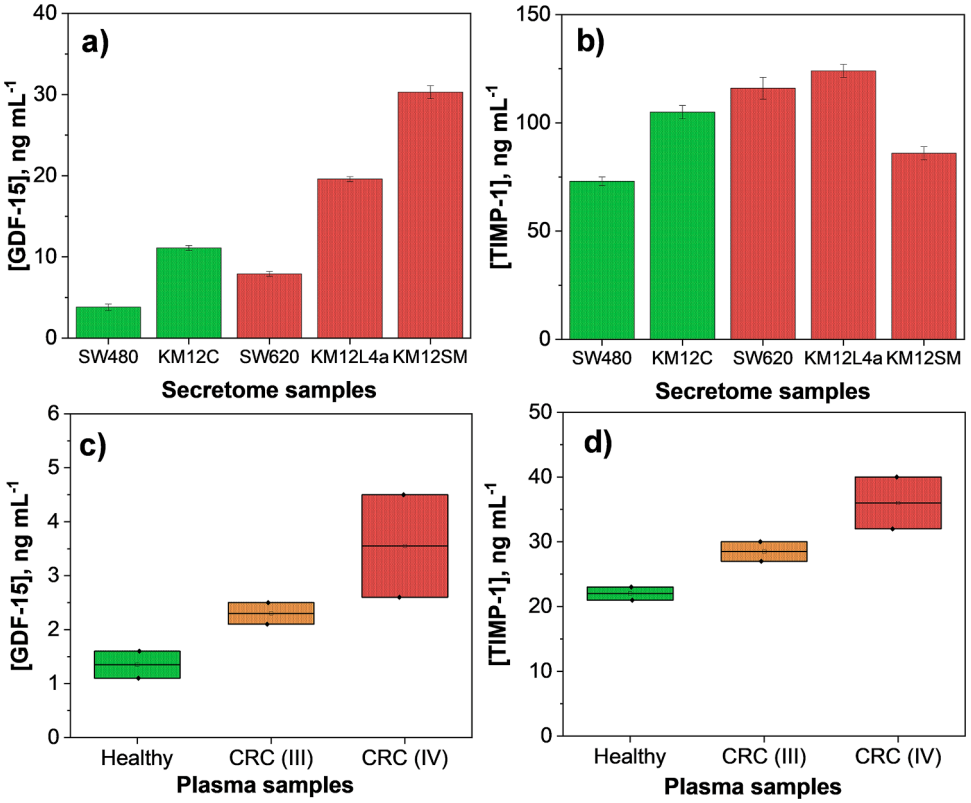


**Fig. 7.** Concentrations of GDF-15 and TIMP-1 in cell secretomes (NM in green and M in red) (a, b) and plasma (healthy individuals in green and CRC patients in stages III in orange or IV in red) (c, d) samples, obtained using the dual immunoplatform.

SW620, KM12SM, and KM12L4a cells in contrast to their corresponding poorly metastatic counterparts. However, the TIMP-1 concentration was found increased only in the metastatic SW620 and KM12L4a CRC cells in comparison to their corresponding low metastatic counterparts and to the highly metastatic to liver KM12SM cells. These results agreed with those obtained by Dot-Blot analysis for the SW CRC cells secretome (Fig. 6**b**). However, the increased levels of TIMP-1 in the secretome of KM12L4a cells was not observed by Dot-Blot, which might be due to the hook effect associated because of the high level of this protein in the KM12L4a cells' secretome.

On the other hand, as no matrix effect was observed for the single determination of TIMP-1 and GDF-15 in plasma samples with the respective immunoplatforms, their quantification with the dual platform was performed by interpolating the sample signals into the calibration plots built with the respective protein standards after a simple sample dilution (1/250 for TIMP-1 and 1/25 for GDF-15 [18]).

The results obtained for the dual determination of both biomarkers in the analyzed samples are displayed in Fig. 7 and summarized in Table 3.

As shown in Figs. 7**c and** 7**d**, larger concentrations of both biomarkers were found in plasma samples of CRC patients compared to those determined for healthy individuals, thus allowing us to discern between healthy individuals and CRC patients. Furthermore, larger concentrations were observed at advanced stages (III *vs.* IV), which agrees with the increase reported in the serological concentration of GDF-15 [59,71,72] and TIMP-1 [20,24,25,27,31,50,73,74,75,76] with the stages of CRC advancement. In addition, the concentrations found in plasma samples for GDF-15 were pretty similar to those reported previously for CRC patients [18,59,60]. Regarding the TIMP-1 concentrations found, they were lower than those reported by Ishida et al. [25], but close to those given by Nielsen et al. [75], which can be attributed to the nature of every sample. In addition, it has been claimed that TIMP-1 serum concentrations are correlated with nodal involvement, presence of distant metastases, patients' survival, and tumor resectability [20, 41].

This work reports the first results described in literature for the determination of GDF-15 and TIMP-1 in cell secretome samples (Figs. 7**a** and 7**b**), and allowed differentiation between non-metastatic and metastatic samples, as previously reported in literature for other biomarkers [61,77,78].

Moreover, recovery studies made for both biomarkers in the analyzed samples provided values between 100–102 %, when a representative sample of each pool was spiked with 250 pg $mL^{-1}$ of the target biomarkers (**Table S6** in the Supplementary Material). These values demonstrated the accuracy and reproducibility of the methodology developed for the simultaneous determination of GDF-15 and TIMP-1, even in highly complex biological samples.

### *3.4.3. Diagnostic ability of TIMP-1 and GDF-15 for CRC*

To assess the diagnostic ability of TIMP-1 and GDF-15 in CRC, we made ROC curves analyses with the data obtained with the dual immunoplatform (Fig. 8). Both proteins were able to significantly discriminate KM12 and SW highly metastatic cells in cell extracts and secretomes with an area under the curve (AUC), sensitivity, and specificity of 100 %. However, TIMP-1 levels in the secretome of KM12 cells were not able to distinguish the metastatic potential of the cells (Fig. 8**a**). In addition, TIMP-1 and GDF-15 levels in plasma and tissue samples significantly discriminated tumoral samples from healthy samples with full diagnostic ability of CRC (AUC, sensitivity, and specificity of 100 %) (Fig. 8**b**). The very favorable values of these parameters were attributed to the selected markers, the nature of the samples, and the cohort of patients analyzed, which, although small, we consider to be extreme (healthy subjects and patients with CRC in advanced stages -stages III and IV-).

## 4. Conclusions

This paper reports the first electrochemical immunoplatforms for the individual determination of TIMP-1 and for the dual determination of TIMP-1 and GDF-15, two biomarkers of emerging relevance related to cellular senescence and diagnosis and prognosis of CRC. Both immunoplatforms rely on sandwich immunoassays using magnetic microsupports and specific antibodies to capture and detect the target biomarkers at disposable screen-printed single or dual detection electrodes and employing amperometric transduction with the $H_2O_2$/HRP/HQ system. Antibodies from ELISA kits recommended for TIMP-1 or GDF-15 determination in cell culture supernatant, serum, and plasma have been used with reliable results even in cell and tissue extracts. The outstanding analytical performance of the developed immunoplatforms allow their application in the analysis of small amounts of an appealing variety of highly complex relevant clinical samples. Thereupon, the usefulness of the immunoplatform for the single determination of TIMP-1 was assessed through the analysis of 0.10 μg of tissue samples and 0.25 μg of protein extracts, while the suitability of the dual immunoplatform was demonstrated through the analysis of 1/25 (GDF-15) or 1/250 (TIMP-1) diluted plasma and secretome samples. Both immune platforms are able to distinguish between liquid samples from healthy individuals and CRC patients and between tumoral and non-tumoral adjacent solid samples in very short times (~ 1 h), using simple protocols and minimum amounts of biological material. The developed methodology involves cost-effective electrochemical instrumentation compatible with routine analysis and, if needed, with portable systems that would allow on-site measurements to continue advancing in the understanding and therefore in the precision of the diagnosis, prognosis and treatment of CRC.

## CRediT authorship contribution statement

**Sandra Tejerina-Miranda:** Methodology, Investigation, Writing – review & editing, Writing – original draft. **Maria Gamella:**

**Table 3**
Results obtained in the analysis of plasma and cell secretome samples using the developed dual immunoplatform for the simultaneous determination of GDF-15 and TIMP-1.

| Biological sample | | | [GDF-15], ng $mL^{-1}$* | $RSD_{n=3}$, % | [TIMP-1], ng $mL^{-1}$* | $RSD_{n=3}$, % |
|---|---|---|---|---|---|---|
| Cell secretome | SW480 | | 3.8 ± 0.4 | 3.7 | 73 ± 2 | 1.1 |
| | SW620 | | 7.9 ± 0.3 | 1.3 | 116 ± 5 | 1.7 |
| | KM12C | | 11.1 ± 0.3 | 1.3 | 105 ± 3 | 1.3 |
| | KM12L4a | | 19.6 ± 0.6 | 0.6 | 124 ± 3 | 1.0 |
| | KM12SM | | 30.3 ± 0.8 | 1.0 | 86 ± 3 | 1.2 |
| Plasma | Healthy | 1 | 1.1 ± 0.1 | 4.5 | 23 ± 2 | 2.7 |
| | | 2 | 1.6 ± 0.2 | 4.3 | 21.0 ± 0.4 | 0.8 |
| | CRC (III) | 3 | 2.5 ± 0.3 | 4.6 | 30 ± 2 | 2.9 |
| | | 4 | 2.1 ± 0.2 | 3.2 | 27 ± 1 | 2.1 |
| | CRC | 5 | 2.6 ± 0.1 | 1.8 | 32 ± 2 | 2.9 |
| | (IV) | 6 | 4.5 ± 0.2 | 1.4 | 40 ± 4 | 4.3 |

* *Mean value* ± $ts/\sqrt{n}$; $n = 3$; $\alpha = 0.05$.

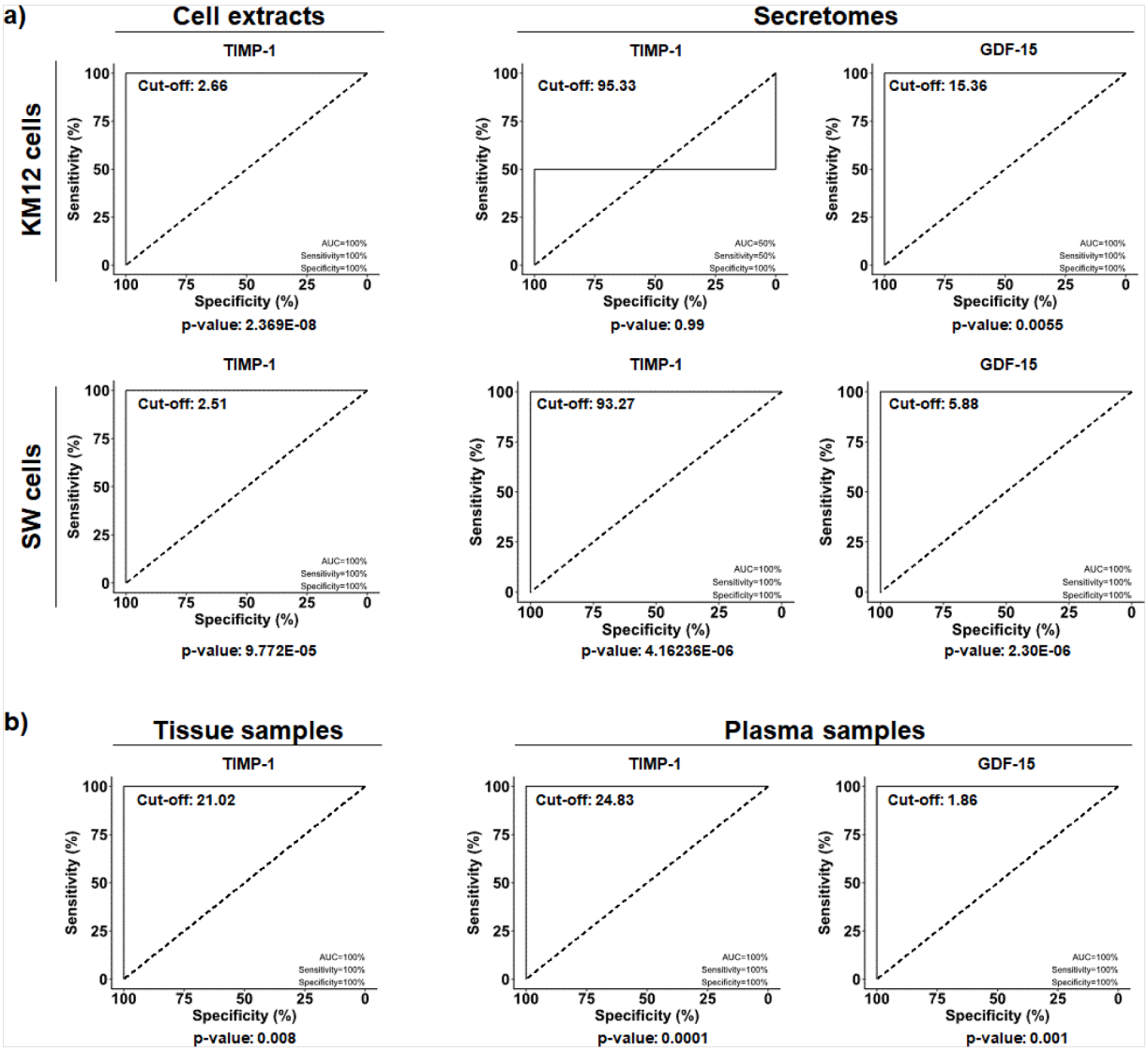


**Fig. 8.** Analysis of the diagnostic ability of TIMP-1 and GDF-15 in cell protein extracts and secretomes (a) from CRC cells, and in plasma and tissue samples (b) from CRC patients and healthy individuals by means of ROC curves analyses.

Methodology, Investigation, Writing – review & editing, Writing – original draft. **María Pedrero:** Supervision, Writing – review & editing, Writing – original draft, Funding acquisition. **Ana Montero-Calle:** Investigation, Writing – review & editing, Writing – original draft. **Raquel Rejas:** Investigation, Writing – review & editing, Writing – original draft. **José M. Pingarrón:** Resources, Writing – review & editing, Writing – original draft. **Rodrigo Barderas:** Conceptualization, Supervision, Resources, Writing – review & editing, Writing – original draft, Funding acquisition. **Susana Campuzano:** Conceptualization, Supervision, Resources, Writing – review & editing, Writing – original draft, Funding acquisition.

## Declaration of competing interest

The authors declare that they have no known competing financial interests or personal relationships that could have appeared to influence the work reported in this paper.

## Data availability

Data will be made available on request.

## Acknowledgements

The financial support of Grants PID2022#x2013;136351OB-I00 and PID2022–140307OB-I00 funded by MCIN/AEI/10.13039/501100011033 and by "ERDF A way of making Europe", EU's Horizon 2020 funding program (UCM's Specific Research Fund FEI-EU-22–08) and PI20CIII/00019 and PI23CIII/00027 grants from the AES-ISCIII program are gratefully acknowledged. S.T.M. acknowledges a predoctoral contract from the Spanish Ministerio de Ciencia e Innovación (PRE2020-092859).

## Supplementary materials

Supplementary material associated with this article can be found, in the online version, at doi:10.1016/j.electacta.2024.144822.

## References

[1] Y. Guo, J.L. Ayers, K.T. Carter, T. Wang, S.K. Maden, D. Edmond, P. Newcomb P, C. Li, C. Ulrich, M. Yu, W.M. Grady, Senescence-associated tissue microenvironment promotes colon cancer formation through the secretory factor GDF15, Aging Cell 18 (2019) e13013, https://doi.org/10.1111/acel.13013.

[2] D. Hanahan, Hallmarks of cancer: new dimensions, Cancer Discov 12 (2022) 31–46, https://doi.org/10.1158/2159-8290.CD-21-1059.

[3] K. Dong, J. Liu, W. Zhou, G. Zhang, Exploring the relationship between senescence and colorectal cancer in prognosis, immunity, and treatment, Front. Genet. 13 (2022) 930248, https://doi.org/10.3389/fgene.2022.930248.

[4] J. Ferlay, M. Ervik, F. Lam, M. Laversanne, M. Colombet, L. Mery, M. Piñeros, A. Znaor, I. Soerjomataram, F. Bray, Global Cancer Observatory: Cancer Today. Lyon, France: International Agency for Research on Cancer. Available from: https://gco.iarc.who.int/today, accessed [8 June 2024].

[5] F.A. Macrae, Epidemiology and risk factors for colorectal cancer, UpToDate Topic 2606 Version 123.0 (2024), https://www.uptodate.com/contents/epidemiology-and-risk-factors-for-colorectal-cancer#, accessed [8 June 2024].

[6] American Cancer Society. Colorectal cancer early detection, diagnosis, and staging. 2020, https://www.cancer.org/cancer/types/colon-rectal-cancer/detection-diagnosis-staging.html, accessed [8 June 2024].

[7] K. Chen, G. Collins, H. Wang, J.W.T. Toh, Pathological features and prognostication in colorectal cancer, Curr. Oncol. 28 (2021) 5356–5383, https://doi.org/10.3390/curroncol28060447.

[8] M.M. Petersen, J. Kleif, L.N. Jørgensen, J.W. Hendel, J.B. Seidelin, M.R. Madsen, J. Vilandt, S. Brandsborg, J.S. Rasmussen, L.M. Andersen, A. Khalid, L. Ferm, S. H. Gawel, F. Martens, B. Andersen, M. Rasmussen, G.J. Davis, I.J. Christensen, C. Therkildsen, Optimizing screening for colorectal cancer: an algorithm combining fecal immunochemical test, blood-based cancer-associated proteins and demographics to reduce colonoscopy burden, Clin. Colorectal Cancer 22 (2) (2023) 199–210, https://doi.org/10.1016/j.clcc.2023.02.001.

[9] H.M. Kluger, K. Hoyt, A. Bacchiocchi, T. Mayer, J. Kirsch, Y. Kluger, M. Sznol, S. Ariyan, A. Molinaro, R. Halaban, Plasma markers for identifying patients with metastatic melanoma, Clin. Cancer Res. 17 (8) (2011) 2417–2425, https://doi.org/10.1158/1078-0432.CCR-10-2402.

[10] W. Du, A. Piek, E.M. Schouten, C.W.A. van de Kolk, C. Mueller, A. Mebazaa, A. A. Voors, R.A. de Boer, H.H.W. Silljé, Plasma levels of heart failure biomarkers are primarily a reflection of extracardiac production, Theranostics 8 (15) (2018) 4155–4169, https://doi.org/10.7150/thno.26055.

[11] Y. Gao, X. Bai, J. Lu, L. Zhang, X. Yan, X. Huang, H. Dai, Y. Wang, L. Hou, S. Wang, A. Tian, J. Li, Prognostic value of multiple circulating biomarkers for 2-year death in acute heart failure with preserved ejection fraction, Front. Cardiovasc. Med. 8 (2021) 779282, https://doi.org/10.3389/fcvm.2021.779282.

[12] X. Liu, S. Pan, V. Xanthakis, R.S. Vasan, B.M. Psaty, T.R. Austin, A.B. Newman, J. L. Sanders, C. Wu, R.P. Tracy, R.E. Gerszten, M.C. Odden, Plasma proteomic signature of decline in gait speed and grip strength, Aging Cell 21 (2022) e13736, https://doi.org/10.1111/acel.13736.

[13] K. McDowell, R. Campbell, J. Simpson, J.W. Cunningham, A.S. Desai, P.S. Jhund, M.P. Lefkowitz, J.L. Rouleau, K. Swedberg, M.R. Zile, S.D. Solomon, M. Packer, J.J. V. McMurray, Incremental prognostic value of biomarkers in PARADIGM-HF, Eur. J. Heart Failure 25 (2023) 1406–1414, https://doi.org/10.1002/ejhf.2887.

[14] Y. Wang, T. Jiang, M. Jiang, S. Gu, Appraising growth differentiation factor 15 as a promising biomarker in digestive system tumors: a meta-analysis, BMC Cancer 19 (2019) 177, https://doi.org/10.1186/s12885-019-5385-y.

[15] S. Mielcarska, K. Stopińska, M. Dawidowicz, A. Kula, P. Kiczmer, A.P. Seńkowska, E.N. Zajdel, K. Walkiewicz, D. Waniczek, E. Świętochowska, GDF-15 level correlates with CMKLR1 and VEGF-A in tumor-free margin in colorectal cancer, Curr. Med. Sci. 41 (3) (2021) 522–528, https://doi.org/10.1007/s11596-021-2335-0.

[16] C. Li, X. Wang, J.I. Casal, J. Wang, P. Li, W. Zhang, E. Xu, M. Lai, H. Zhang, Growth differentiation factor 15 is a promising diagnostic and prognostic biomarker in colorectal cancer, J. Cell. Mol. Med. 20 (8) (2016) 1420–1426, https://doi.org/10.1111/jcmm.12830.

[17] I.F. Kamel, H.M. Elsadek, A. Mokhtar Ahmad, A.I. Elagrody, Value of serum growth differentiation factor 15 in diagnosis of colorectal cancer, Egypt. J. Hosp. Med. 85 (2) (2021) 3639–3644.

[18] S. Tejerina-Miranda, V. Pérez-Ginés, R.M. Torrente-. Rodríguez, M. Pedrero, A. Montero-Calle, J.M. Pingarrón, R. Barderas, S. Campuzano, Magneto-controlled electrochemical immunosensing platform to assess the senescence-associated GDF-15 marker in colorectal cancer, Sens. Diagn. 3 (2024) 238–247, https://doi.org/10.1039/d3sd00311f.

[19] N. Yukawa, T. Yoshikawa, M. Akaike, Y. Sugimasa, Y. Rino, M. Masuda, T. Imada, Impact of plasma tissue inhibitor of matrix metalloproteinase-1 on long-term survival in patients with colorectal cancer, Oncology 72 (2007) 205–208, https://doi.org/10.1159/000112827.

[20] B. Mroczko, M. Groblewska, B. Kedra, B. Okulczyk, M. Szmitkowski, The diagnostic value of matrix metalloproteinase 9 (MMP-9) and tissue inhibitor of matrix metalloproteinases 1 (TIMP-1) determination in the sera of colorectal adenoma and cancer patients, Int. J. Colorectal Dis. 25 (2010) 1177–1184, https://doi.org/10.1007/s00384-010-0991-9.

[21] M. Łukaszewicz-Zajac, B. Mroczko, Circulating biomarkers of colorectal cancer (CRC)—Their utility in diagnosis and prognosis, J. Clin. Med. 10 (2021) 2391, https://doi.org/10.3390/jcm10112391.

[22] I. Guccini, A. Revandkar, M. D'Ambrosio, M. Colucci, E. Pasquini, S. Mosole, M. Troiani, D. Brina, R. Sheibani-Tezerji, A.R. Elia, A. Rinaldi, N. Pernigoni, J. H. Rüschoff, S. Dettwiler, A.M. De Marzo, E.S. Antonarakis, C. Borrelli, A.E. Moor, R. Garcia-Escudero, A. Alajati, G. Attanasio, M. Losa, H. Moch, P. Wild, G. Egger, A. Alimonti, Senescence reprogramming by TIMP1 deficiency promotes prostate cancer metastasis, Cancer Cell 39 (1) (2021) 68–82, https://doi.org/10.1016/j.ccell.2020.10.012.

[23] A. Katoch, D. Nayak, M.M. Faheem, A. Kumar, P.K. Sahu, A.P. Gupta, L.D. Kumar, A. Goswami, Natural podophyllotoxin analog 4DPG attenuates EMT and colorectal cancer progression via activation of checkpoint kinase 2, Cell Death Discov. 7 (2021) 25, https://doi.org/10.1038/s41420-021-00405-3.

[24] M.N. Holten-Andersen, G. Murphy, H.J. Nielsen, A.N. Pedersen, I.J. Christensen, G. Høyer-Hansen, N. Brünner, R.W. Stephens, Quantitation of TIMP-1 in plasma of healthy blood donors and patients with advanced cancer, Br. J. Cancer 80 (1999) 495–503, https://doi.org/10.1038/sj.bjc.6690384.

[25] H. Ishida, N. Murata, Y. Hayashi, M. Tada, D. Hashimoto, Serum levels of tissue inhibitor of metalloproteinases-1 (TIMP-1) in colorectal cancer patients, Surg. Today 33 (2003) 885–892, https://doi.org/10.1007/s00595-003-2628-x.

[26] M.N. Holten-Andersen, C. Fenger, H.J. Nielsen, A.-S.S. Rasmussen, I.J. Christensen, N. Brünner, O. Kronborg, Plasma TIMP-1 in patients with colorectal adenomas: a prospective study, Eur. J. Cancer 40 (14) (2004) 2159–2164, https://doi.org/10.1016/j.ejca.2004.06.011.

[27] L. Holten-Andersen, J. Christensen, S.B. Jensen, J. Reibel, S. Laurberg, B. Nauntofte, N. Brümmer, Saliva and plasma TIMP-1 in patients with colorectal cancer: a prospective study, Scand. J. Gastroenterol. 47 (2012) 1234–1241, https://doi.org/10.3109/00365521.2012.711855.

[28] K.-L.G. Spindler, I.J. Christensen, H.J. Nielsen, A. Jakobsen, N. Brünner, TIMP-1 and CEA as biomarkers in third-line treatment with irinotecan and cetuximab for metastatic colorectal cancer, Tumor Biol 36 (2015) 4301–4308, https://doi.org/10.1007/s13277-015-3069-z.

[29] G. Cheng, X. Fan, M. Hao, J. Wang, X. Zhou, X. Sun, Higher levels of TIMP-1 expression are associated with a poor prognosis in triple-negative breast cancer, Mol. Cancer 15 (2016) 30, https://doi.org/10.1186/s12943-016-0515-5.

[30] K. Souček, A. Malenovská, Z. Kahounová, J. Remšík, Z. Holubcová, T. Soukup, D. Kurfürstová, J. Bouchal, T. Suchánková, E. Slabáková, A. Hampl, Presence of growth/differentiation factor-15 cytokine in human follicular fluid, granulosa cells, and oocytes, J. Assist. Reprod. Genet. 35 (8) (2018) 1407–1417, https://doi.org/10.1007/s10815-018-1230-5.

[31] M. Vočka, D. Langer, V. Fryba, J. Petrtyl, T. Hanus, M. Kalousova, T. Zima, L. Petruzelka, Serum levels of TIMP-1 and MMP-7 as potential biomarkers in patients with metastatic colorectal cancer, Int. J. Biol. Markers 34 (3) (2019) 292–301, https://doi.org/10.1177/1724600819866202.

[32] S.R. Ishak, M.M.E. Ganzoury, E.M. Fouda, M.A. Anwar, A.M. Kamal, H.M. Hamza, N.A. Bakry, Serum growth differentiation factor-15 (GDF-15) is a biomarker of cardiac manifestations in children with COVID-19, Eur. J. Med. Res. 28 (1) (2023) 527, https://doi.org/10.1186/s40001-023-01514-8.

[33] G. Song, S. Xu, H. Zhang, Y. Wang, C. Xiao, T. Jiang, L. Wu, T. Zhang, X. Sun, L. Zhong, C. Zhou, Z. Wang, Z. Peng, J. Chen, X. Wang, TIMP1 is a prognostic marker for the progression and metastasis of colon cancer through FAK-PI3K/AKT and MAPK pathway, J. Exp. Clin. Cancer Res 35 (2016) 148, https://doi.org/10.1186/s13046-016-0427-7.

[34] M. Wörnle, M. Roeder, M. Sauter, A. Ribeiro, Role of matrix metalloproteinases in viral-associated glomerulonephritis, Nephrol. Dial. Transplant. 24 (2009) 1113–1121, https://doi.org/10.1093/ndt/gfn627.

[35] A. Tokarzewicz, L. Romanowicz, I. Svekloc, E. Gorodkiewicza, The development of a matrix metalloproteinase-1 biosensor based on the surface plasmon resonance imaging technique, Anal. Meth. 8 (2006) 6428–6435, https://doi.org/10.1039/C6AY01856D.

[36] J. Thevenard, L. Verzeaux, J. Devy, N. Etique, A. Jeanne, C. Schneider, C. Hachet, G. Ferracci, M. David, L. Martiny, E. Charpentier, M. Khrestchatisky, S. Rivera, S. Dedieu, H. Emonard, Low-density lipoprotein receptor-related protein-1 mediates endocytic clearance of tissue inhibitor of metalloproteinases-1 and promotes its cytokine-like activities, PLoS ONE 9 (7) (2014) e103839, https://doi.org/10.1371/journal.pone.0103839.

[37] C. Lin, S. Liang, Y. Li, Y. Peng, Z. Huang, Z. Li, Y. Yang, X. Luo, Localized plasmonic sensor for direct identifying lung and colon cancer from the blood, Biosens. Bioelectron. 211 (2022) 114372, https://doi.org/10.1016/j.bios.2022.114372.

[38] C. Muñoz-San Martín, V. Pérez-Ginés, R.M. Torrente-Rodríguez, M. Gamella, G. Solís-Fernández, A. Montero-Calle, M. Pedrero, V. Serafín, N. Martínez-Bosch, P. Navarro, P.G. De Frutos, M. Batlle, R. Barderas, J.M. Pingarrón, S. Campuzano, Electrochemical immunosensing of Growth arrest-specific 6 in human plasma and tumor cell secretomes, Electrochem. Sci. Adv. 2 (4) (2021) e2100096, https://doi.org/10.1002/elsa.202100096.

[39] C. Muñoz-San Martín, A. Montero-Calle, M. Garranzo-Asensio, M. Gamella, V. Perez-Gines, M. Pedrero, J.M. Pingarrón, R. Barderas, N. de-los-Santos-Alvarez, M.J. Lobo-Castanon, S. Campuzano, First bioelectronic immunoplatform for quantitative secretomic analysis of total and metastasis-driven glycosylated haptoglobin, Anal. Bioanal. Chem. 415 (2023) 2045–2057, https://doi.org/10.1007/s00216-022-04397-6.

[40] M. Blázquez-García, J. Quinchia, V. Ruiz-Valdepeñas Montiel, R.M. Torrente-Rodríguez, V. Serafín, M. Garranzo-Asensio, A. García-Romero, J. Orozco, R. Barderas, J.M. Pingarrón, S. Campuzano, Electroanalytical immunotool to determine matricellular protein periostin, a stromal biomarker of prognosis in colorectal cancer, ChemElectroChem 11 (2024) e202300641, https://doi.org/10.1002/celc.202300641.

[41] M. Chen, L. Zhao, D. Wu, S. Tu, C. Chen, H. Guo, Y. Xu, Highly sensitive sandwich-type immunosensor with enhanced electrocatalytic durian-shaped $MoS_2$/AuPtPd nanoparticles for human growth differentiation factor-15 detection, Anal. Chim. Acta 1223 (2022) 340194, https://doi.org/10.1016/j.aca.2022.340194.

[42] C. Chen, J. Kang, S. Wang, S. Chen, H. Guo, M. Chen, An electrochemical immunosensor based on polyaniline microtubules and zinc gallinate for detection of human growth differentiation factor-15, Microchim. Acta 190 (2023) 92, https://doi.org/10.1007/s00604-023-05674-6.

[43] M. Chen, Y. Jiao, C. Chen, Y. Wang, H. Lu, X. Dai, A sandwich-type electrochemical immunosensor prepared with graphyne-Au triangular nanoprisms and $MoS_2$-AuPtCu hexagonal nanoframes for the detection of human growth/differentiation factor 15, Microchem. J. 193 (2023) 109150, https://doi.org/10.1016/j.microc.2023.109150.
[44] Y. Jiao, Z. Huang, M. Chen, X. Zhou, H. Lu, B. Wang, X. Dai, A label-free amperometric immunosensor with improved electrocatalytic 3D braided AuPtCu-SWCNTs@$MoS_2$-rGO for human growth differentiation factor-15 detection, Methods 14 (2022) 1420–1429, https://doi.org/10.1039/D1AY02198B.
[45] S. Fortunati, M. Giannetto, C. Giliberti, M. Mattarozzi, A. Bertucci, M. Careri, Magnetic beads as versatile tools for electrochemical biosensing platforms in point-of-care testing, Anal. Sens. 4 (2024) e202300062, https://doi.org/10.1002/anse.202300062.
[46] J. Quinchia, M. Blázquez-García, R.M. Torrente-Rodríguez, V. Ruiz-Valdepeñas Montiel, V. Serafín, R. Rejas-González, A. Montero-Calle, J. Orozco, J. M. Pingarrón, R. Barderas, S. Campuzano, Disposable electrochemical immunoplatform to shed light on the role of the multifunctional glycoprotein TIM-1 in cancer cells invasion, Talanta 267 (2024) 125155, https://doi.org/10.1016/j.talanta.2023.125155.
[47] J.R. Wiśniewski, F.Z. Gaugaz, Fast and sensitive total protein and peptide assays for proteomic analysis, Anal. Chem. 87 (8) (2015) 4110–4116, https://doi.org/10.1021/ac504689z.
[48] U. Eletxigerra, J. Martínez-Perdiguero, S. Merino, R. Villalonga, J.M. Pingarrón, S. Campuzano, Amperometric magnetoimmunoassay for the direct detection of tumor necrosis factor alpha biomarker in human serum, Anal. Chim. Acta 838 (2014) 37–44, https://doi.org/10.1016/j.aca.2014.05.047.
[49] M. Eguílaz, M. Moreno-Guzmán, S. Campuzano, P. Yáñez-Sedeño, P. Yáñez-Sedeño, J.M. Pingarrón, An electrochemical immunosensor for testosterone using functionalized magnetic beads and screen-printed carbon electrodes, Biosens. Bioelectron. 26 (2) (2010) 517–522, https://doi.org/10.1016/j.bios.2010.07.060.
[50] C. Meng, X. Yin, J. Liu, K. Tang, H. Tang, J. Liao, TIMP-1 is a novel serum biomarker for the diagnosis of colorectal cancer: a metaanalysis, PLoS ONE 13 (11) (2018) e0207039, https://doi.org/10.1371/journal.pone.0207039.
[51] K. Niewiarowska, A. Pryczynicz, V. Dymicka-Piekarska, M. Gryko, D. Cepowicz, W. Famulski, A. Kemonä, K. Guzińska-Ustymowicz, Diagnostic significance of TIMP-1 level in serum and its immunohistochemical expression in colorectal cancer patients, Pol. J. Pathol. 4 (2014) 296–304, https://doi.org/10.5114/pjp.2014.48191.
[52] S. Campuzano, R. Barderas, R.M. Moreno-Casbas, A. Almeida, J.M. Pingarrón, Pursuing precision in medicine and nutrition: the rise of electrochemical biosensing at the molecular level, Anal. Bioanal. Chem. 416 (2024) 2151–2172, https://doi.org/10.1007/s00216-023-04805-5.
[53] S. O'Connor, L.A. Hassan, G. Brennan, K.J. McCarthy, C. Silien, N. Liu, T. Kennedy, K.M. Ryan, E.J. O'Reilly, Cadmium selenide sulfide quantum dots with tuneable emission profiles: an electrochemiluminescence platform for the determination of TIMP-1 protein, Bioelectrochemistry 148 (2022) 108221, https://doi.org/10.1016/j.bioelechem.2022.108221.
[54] F. Deiss, C.N. LaFratta, M. Symer, T.M. Blicharz, N. Sojic, D.R. Walt, Multiplexed sandwich immunoassays using electrochemiluminescence imaging resolved at the single bead level, J. Am. Chem. Soc. 131 (2009) 6088–6089, https://doi.org/10.1021/ja901876z.
[55] F.J. Gruhl, K. Länge, Surface modification of an acoustic biosensor allowing the detection of low concentrations of cancer markers, Anal. Biochem. 420 (2012) 188–190, https://doi.org/10.1016/j.ab.2011.10.006.
[56] D.V. Grigorieva, I.V. Gorudko, A.V. Sokolov, O.V. Kosmachevskaya, A.F. Topunov, I.V. Buko, E.E. Konstantinova, S.N. Cherenkevich, O.M. Panasenko, Measurement of plasma hemoglobin peroxidase activity, Bull. Exp. Biol. Med. 155 (1) (2013) 118–121, https://doi.org/10.1007/s10517-013-2095-3.
[57] S. Dimić-Janjić, M.A. Hoda, B. Milenković, J. Kotur-Stevuljevic, M. Stjepanović, D. Gompelmann, J. Janković, M. Miljković, J. Milin-Lazović, N. Djurdjevic, D. Marić, I. Milivojevic, S. Popević, The usefulness of MMP-9, TIMP-1 and MMP-9/TIMP-1 ratio for diagnosis and assessment of COPD severity, Eur. J. Med. Res. 28 (2023) 127, https://doi.org/10.1186/s40001-023-01094-7.
[58] S. Tvorynska, A. Civera, M. Gamella, R.M. Torrente-Rodríguez, M. Pedrero, P. Galán-Malo, L. Mata, L. Sánchez, J. Barek, J.M. Pingarrón, M.D. Pérez, S. Campuzano, Electrochemical immunosensing of walnut and hazelnut allergenic proteins in processed foods, Sens. Bio-Sens. Res. 44 (2024) 100644, https://doi.org/10.1016/j.sbsr.2024.100644.
[59] C. Li, X. Wang, J.I. Casal, J. Wang, P. Li, W. Zhang, E. Xu, M. Lai, H. Zhang, Growth differentiation factor 15 is a promising diagnostic and prognostic biomarker in colorectal cancer, J. Cell. Mol. Med. 20 (8) (2016) 1420–1426, https://doi.org/10.1111/jcmm.12830.
[60] X. Wang, Z. Yang, H. Tian, Y. Li, M. Li, W. Zhao, Z. Chao, T. Wang, J. Liu, A. Zhang, D. Shen, C. Zheng, J. Qi, D. Zhao, J. Shi, L. Jin, J. Rao, W. Zhang, Circulating MIC-1/GDF15 is a complementary screening biomarker with CEA and correlates with liver metastasis and poor survival in colorectal cancer, Oncotarget 8 (15) (2017) 24892–24901, https://doi.org/10.18632/oncotarget.15279.
[61] R.E. Hewitt, K.E. Brown, M. Corcoran, W.G. Stetler-Stevenson, Increased expression of tissue inhibitor of metalloproteinases type 1 (TIMP-1) in a more tumourigenic colon cancer cell line, J. Pathol. 192 (2000) 455–459, https://doi.org/10.1002/1096-9896(2000)9999:9999≤::AID-PATH777≥3.0.CO;2-E.
[62] H.A. Ree, V.A. Florenes, J.P. Berg, G.M. Maelandsmo, J.M. Nesland, O. Fodstad, High levels of messenger RNAs for tissue inhibitors of metalloproteinases (TIMP-1 and TIMP-2) in primary breast carcinomas are associated with development of distant metastases, Clin. Cancer Res. 3 (1997) 1623–1628.
[63] Z.S. Wu, Q. Wu, J.H. Yang, H.Q. Wang, X.D. Ding, F. Yang, X.C. Xu, Prognostic significance of MMP-9 and TIMP-1 serum and tissue expression in breast cancer, Int. J. Cancer 122 (2008) 2050–2056, https://doi.org/10.1002/ijc.23337.
[64] A.S. Schrohl, V. Mueller, I.B. Christensen, K. Pantel, C. Thomssen, N. Bruenner, A comparative study of tissue inhibitor of metalloproteinases-1 levels in plasma and tumour tissue from patients with primary breast cancer and in plasma from patients with metastatic breast cancer, Tumor. Biol. 29 (2008) 181–187, https://doi.org/10.1159/000146863.
[65] K.M. Fong, Y. Kida, P.V. Zimmerman, P.J. Smith, TIMP1 and adverse prognosis in non-small cell lung cancer, Clin. Cancer Res. 2 (1996) 1369–1372.
[66] T. Yoshikawa, A. Tsuburaya, O. Kobayashi, M. Sairenji, H. Motohashi, S. Yanoma, Y. Miyagi, Intratumoral concentrations of tissue inhibitor of matrix metalloproteinase 1 in patients with gastric carcinoma, A new biomarker for invasion and its impact on survival, Cancer 91 (2001) 1739–1744, https://doi.org/10.1002/1097-0142(20010501)91:9≤1739::aid-cncr1192≥3.0.co;2-9.
[67] T. Yoshikawa, A. Tsuburaya, O. Kobayashi, M. Sairenji, Y. Miyagi, Protein levels of tissue inhibitor of metalloproteinase-1 in tumor extracts as a marker for prognosis and recurrence in patients with gastric cancer, Gastric Cancer 9 (2) (2006) 106–113, https://doi.org/10.1007/s10120-006-0362-y.
[68] R.E. Hewitt, I.H. Leach, D.G. Powe, I.M. Clark, T.E. Cawston, D.R. Turner, Distribution of collagenase and tissue inhibitor of metalloproteinases (TIMP) in colorectal tumours, Int. J. Cancer 49 (1991) 666–672, https://doi.org/10.1002/ijc.2910490507.
[69] E.A. Baker, F.G. Bergin, D.J. Leaper, Matrix metalloproteinases, their tissue inhibitors and colorectal cancer staging, Br. J. Surg. 87 (2000) 1215–1221, https://doi.org/10.1046/j.1365-2168.2000.01531.x.
[70] M.N. Holten-Andersen, U. Hansen, N. Brünner, H.J. Nielsen, M. Illemann, B. S. Nielsen, Localization of tissue inhibitor of metalloproteinases 1 (TIMP-1) in human colorectal adenoma and adenocarcinoma, Int. J. Cancer 113 (2) (2004) 198–206, https://doi.org/10.1002/ijc.20566.
[71] U. Wallin, B. Glimelius, K. Jirström, S. Darmanis, R.Y. Nong, F. Pontén, C. Johansson, L. Påhlman, H. Birgisson, Growth differentiation factor 15: a prognostic marker for recurrence in colorectal cancer, Br. J. Cancer 104 (2011) 1619–1627, https://doi.org/10.1038/bjc.2011.112.
[72] K. Jakubowska, A. Pryczynicz, V. Dymicka-Piekarska, D. Cepowicz, D. Jagodzińska, Ł. Lewczuk, A. Lebelt, M. Ozimkiewicz, P. Kiszło, K. Guzińska-Ustymowicz, The growth differentiation factor-15 (GDF-15) can be useful in the detection of distant metastases in sera of colorectal cancer patients, Prog. Health Sci. 6 (1) (2016) 40–48, https://doi.org/10.5604/01.3001.0009.5108.
[73] M.N. Holten-Andersen, I.J. Christensen, G. Høyer-Hansen, H. Lilja, G. Murphy, V. Jensen, N. Brünner, T. Piironen, Measurement of the noncomplexed free fraction of tissue inhibitor of metalloproteinases 1 in plasma by immunoassay, Clin. Chem. 48 (8) (2002) 1305–1313, https://doi.org/10.1093/clinchem/48.8.1305.
[74] E.T. Waas, T. Hendriks, R.M.L.M. Lomme, T. Wobbes, Plasma levels of matrix metalloproteinase-2 and tissue inhibitor of metalloproteinase-1 correlate with disease stage and survival in colorectal cancer patients, Dis. Colon Rectum 48 (2005) 700–710, https://doi.org/10.1007/s10350-004-0854-y.
[75] H.J. Nielsen, N. Brünner, L.N. Jorgesen, J. Olsen, H.B. Rahr, K. Thygesen, U. Hoyer, S. Laurberf, P. Stieber, M.A. Blankenstein, G. Davis, B.L. Dowell, J. Christensen, Plasma TIMP-1 and CEA in detection of primary colorectal cancer: a prospective, population based study of 4509 high-risk individuals, Scand. J. Gastroenterol. 46 (2011) 60–69, https://doi.org/10.3109/00365521.2010.513060.
[76] C. Böckelman, I. Beilmann-Lehtonen, T. Tuomas Kaprio, S. Koskensalo, T. Tervahartiala, H. Mustonen, U. Stenman, T. Timo Sorsa, C. Haglund, Serum MMP-8 and TIMP-1 predict prognosis in colorectal cancer, BMC Cancer 18 (2018) 679, https://doi.org/10.1186/s12885-018-4589-x.
[77] H. Xue, B. Lü, J. Zhang, M. Wu, Q. Huang, Q. Wu, H. Sheng, D. Wu, J. Hu, M. Lai, Identification of serum biomarkers for colorectal cancer metastasis using a differential secretome approach, J. Proteome Res. 9 (1) (2009) 545–555, https://doi.org/10.1021/pr9008817.
[78] H. Feng, L. Chen, Q. Wang, B. Shen, L. Liu, P. Zheng, S. Xu, X. Liu, J. Chen, T. Jiang, Calumenin-15 facilitates filopodia formation by promoting TGF-β superfamily cytokine GDF-15 transcription, Cell Death Dis. 4 (10) (2013) e870, https://doi.org/10.1038/cddis.2013.403.